Audio Engineering Society

Conference Paper 62

Presented at the International Conference on Spatial and Immersive Audio
2023 August 23–25, Huddersfield, UK

Miniature Line Array for Immersive Sound Reinforcement

Lukas Gölles[1,2], Franz Zotter[1,2], and Leon Merkel[2,3]

[1] *Institute of Electronic Music and Acoustics, Graz, Austria*
[2] *University of Music and Performing Arts, Graz, Austria*
[3] *Graz, University of Technology, Austria*

Correspondence should be addressed to Lukas Gölles (goelles@iem.at)

ABSTRACT

Progressively curved line-source arrays became state of the art in large-scale sound reinforcement as they are flexibly adapted to the listening area by well-chosen splay angles between individual elements in the chain of line-source loudspeakers. In cinema-sized sound reinforcement, point-source loudspeaker setups are still common, despite maybe difficult to adjust to designs targets suggested by current literature: 0 dB per doubling of the distance for ideally preserved direct sound mix, -3 dB per doubling of the distance for ideally preserved envelopment. To explore how much practical benefit lies in pursuing these targets with smaller line arrays, this paper presents the open design for a miniature line array with 3D printed enclosure. Moreover, measured free field frequency responses, distortion, and directvity are discussed for an individual prototype element, and of the entire line array the coverage over distance is discussed for two target designs using a purely curved or curved and delayed array.

1 Introduction

One of the big challenges for sound reinforcement in concerts, cinema, or speech events is to provide high-quality sound for the largest parts of a predefined audience area [1]. For immersive sound reinforcement, Zotter et. al [2] showed that acceptable mixing balance of direct sound objects is achieved when rendered with -1 dB roll-off per doubling of the distance and Gölles et. al [3] showed that loudspeakers, designed for a direct-sound coverage of 0 dB attenuation per doubling of the distance, could potentially improve directional localisation in a large listening area, above a length-dependent frequency. Considering envelopment of a diffuse scene, Riedel et al. [4, 5] purposes to use horizontally surround loudspeakers whose sound level decrease with -3 dB per doubling of the distance.

Variable curvature line arrays seem to be suitable to implement these designs in practise. For example, the Wavefront Sculpture Technology [6, 7] defines the curvature of line source arrays to adjust the direct sound level for a predefined listening area. Furthermore, a Straube et al define an algorithm to optimize the tilt angles between the individual elements of a line source array [8]. What literature has in common is that only one target design is pursued.

Considering optimal mixing balance and optimally pre-

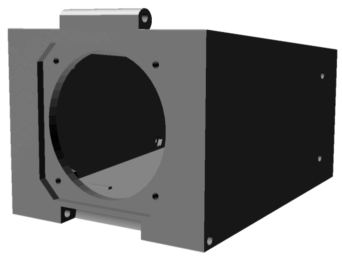

Fig. 1: CAD model of a single cabinet.

serving the envelopment for off-center listening positions, current knowledge suggests a two-target design. The practical goal is to use only one loudspeaker array to satisfy both targets.

This paper presents the open design of a 3D printed miniature line array element that joins with others and permits to adjust a splay angles in between. The primary target is to implement an experimental setup to accomplish multiple target designs for cinema-sized sound reinforcement. The primary target is reached by adjusting the splay angles between the individual elements which are driven in phase. Individual delays added in each loudspeaker feed of the array allow other targets to be met on another signal bus. Beside the open design, impulse response measurements are presented to show the practical performance of the prototype.

2 Design of the loudspeaker element

The line array should be small enough to reach a high spatial aliasing limit, and it should be able to cover a wide frequency range. To accomplish this while keeping the technical effort manageable, a solution of broad-band loudspeakers (1-way system) of small size is preferable. We chose SB acoustics SB65WBAC25-4[1] as wide-band transducer as implemented by the 3|9|3 loudspeaker [9] because of their ability to reproduce low frequencies from 115 Hz on and to perform with high quality also at high frequencies.

The resonance frequency is calculated by the compliance $C_{\mathrm{ms}} = 0.77\,\frac{\mathrm{mm}}{\mathrm{N}}$ and the moving mass $M_{\mathrm{ms}} = 2.5\,\mathrm{g}$,

$$f_{\mathrm{s}} = \frac{1}{2\pi}\,\frac{1}{\sqrt{C_{\mathrm{ms}}\,M_{\mathrm{ms}}}} = 115\,\mathrm{Hz}. \tag{1}$$

[1] https://sbacoustics.com/product/2-5in-sb65wbac25-4/

Fig. 2: Miniature line array with 3D printed cabinets, fully assembled, 8-element example.

We allow a shift of the resonance frequency by $\sqrt{2}$, so that the resonance frequency of the closed box is $f_{\mathrm{cb}} = 162\,\mathrm{Hz}$ yielding the compliance ratio $\alpha = \frac{f_{\mathrm{cb}}^2}{f_{\mathrm{s}}^2} - 1 = 1$. This defines the volume of the closed box to be equal to the equivalent volume of the driver suspension $V_{\mathrm{as}} = 0.43\,\mathrm{l}$. As the interior of our real box is loosely filled with Visaton Damping Material, the goal is to reach a volume of approximately $V_{\mathrm{as}} = 0.4\,\mathrm{l}$.

To minimise the effect of spatial aliasing, the drivers have to be placed as closely together as possible, yielding a minimum feasible inside front cabinet height $h_{\mathrm{f,i}} = 6.4\,\mathrm{cm}$. 8 mm thick walls have to be added to ensure stability and to enable linking of the cabinet fronts. This results in an outside front cabinet height of $h_{\mathrm{f,o}} = 8\,\mathrm{cm}$. Furthermore, the cabinet side profile must be trapezoidal to permit angular range of motion required to adjust the inclination between the line array elements, cf. Figs. 1 and 2. Setting the maximum adjustable splay angle to 10°, as common in professional sound reinforcement systems, and a cabinet depth of $d_{\mathrm{i}} = 10\,\mathrm{cm}$, yields as back height of the cabinet

$$h_{\mathrm{b,i}} = h_{\mathrm{f,i}} - 2\,d_{\mathrm{i}}\,\tan\left(\frac{10^\circ}{2}\,\frac{\pi}{180^\circ}\right) = 4.65\,\mathrm{cm}, \tag{2}$$

or $h_{\mathrm{b,o}} = 6.25\,\mathrm{cm}$ on the outside. We choose $w_{\mathrm{i}} = 8.4\,\mathrm{cm}$ or $w_{\mathrm{o}} = 10\,\mathrm{cm}$ for the width of the cabinets to provide enough space for cabling. With these dimensions and the volume that is occupied by the driver V_{d}, the interior volume of this trapezoidal prism is

$$V_\mathrm{b} = \frac{h_\mathrm{f,i} + h_\mathrm{b,i}}{2}\, w_\mathrm{i}\, d_\mathrm{i} - V_\mathrm{d} = 404.1\,\mathrm{cm}^3\,. \tag{3}$$

From measurements, we get a resonance frequency of 161 Hz, matching the theoretical considerations.

Figure 1 shows the CAD model of a single enclosure and Figure 2 presents the 3D printed prototype with mounted drivers as exemplary setup with 8 enclosures.

3 Design of line array curvature

Typically, the sound pressure of a linear arrangement of ideal point sources decreases with $1/\sqrt{f}$, cf. Appendix A. The goal in line array curvature design is to reach an equalised magnitude square $8\,\pi\,k\,|p|^2 = \left(\frac{g}{r^\beta}\right)^2$ with adjustable $-6\cdot\beta$ dB per doubling of the distance r between the point on the array emitting the first wave front received and the receiver; $k = \frac{2\pi f}{c}$ is the wave number and $c = 343\,\mathrm{m/s}$ the speed of sound.

The theory of adjusting the splay angles in the chain of line-source loudspeaker arrays is known from the Wavefront Sculpture Technology [6, 7]. In [10], the stationary-phase approximated integral of a Green's function over an unknown contour was used to obtain a more generic differential equation for a total curvature

$$\dot{\vartheta}_\mathrm{T} = -\frac{r^{2\beta}}{g^2}\,\frac{1}{r^2\,\cos\vartheta_\mathrm{w}} + \frac{\cos\vartheta_\mathrm{w}}{r} \qquad r = \frac{z}{\sin\vartheta_\mathrm{T}}\,, \tag{4}$$

which corresponds to the design equation for line source array curvature of the Wavefront Sculpture Technology without beamforming when $\vartheta_\mathrm{w} = 0$ as presented in [6]. Here, the total inclination $\vartheta_\mathrm{T} = a\,\vartheta + (1-a)\,\vartheta_\mathrm{w}$ at any point of the array is linearly composed of the physical inclination ϑ of the curved array contour and a local delay-and-sum beamformer's steering angle ϑ_w. The total curvature $\dot{\vartheta}_\mathrm{T}$ is the total inclination change over the natural length parameter s of the contour. The gain parameter g sets the initial curvature at the highest point of the source. Defining the tangent vector $\boldsymbol{t} = \begin{bmatrix}\sin\vartheta & 0 & \cos\vartheta\end{bmatrix}^\mathsf{T}$, we get the source contour by integration over the natural length parameter $\boldsymbol{x} = \int_0^s \boldsymbol{t}\,\mathrm{d}s$.

To simulate a real case scenario, 12 enclosures are lined up, for which we obtain the continuous source contour from eq. (4). A web-based tool[2] is used to solve the differential equation with low effort yielding discrete splay angles and delays. For simulation, we use the following parameters: The mounting height was set to $z(s=0) = 2\,\mathrm{m}$ and the farthest observation point to $x_{\mathrm{r},0} = 10\,\mathrm{m}$, which defines the gain parameter $g = 0.27$. The solution is then discretized using a step size of 8.2 cm, which corresponds to the distance between two neighbouring drivers when mounted in the chain. For broadside beamforming, this yielding the spatial aliasing frequency for which endfire radiation occurs whenever $\lambda < 8.2\,\mathrm{cm}$,

$$f_\text{spat. al.} = 4.2\,\mathrm{kHz}. \tag{5}$$

The discretized solution yields integer splay angles which are summarised in Table 1.

enclosure	Tilt angle	delay
1	11.3°	0
2	0°	0
3	0°	1
4	1°	1
5	0°	2
6	1°	3
7	1°	4
8	1°	6
9	2°	8
10	3°	10
11	4°	13
12	10°	15

Table 1: Tilt angles for the curved array and delays in samples at $f_s = 48\,\mathrm{kHz}$ for the mixed array

To include effects caused by source discretization, the simulated continuous contour was discretized into a polygon of 6.2 cm straight-line segments leaving gaps in between, as done in [10]. On these polygons, same-delay point sources are positioned and the sound pressures of all point sources are summed up. The dashed lines in Figure 7 show the results for the curved line source without beamforming and $\beta = 0$ as well as the result of the mixed design by adding delays to reach -3 dB per doubling of the distance where a second gain parameter $g = 0.567$ was used for the mixed design.

[2] https://enimso.iem.sh/post/line-array-designer-two-target/

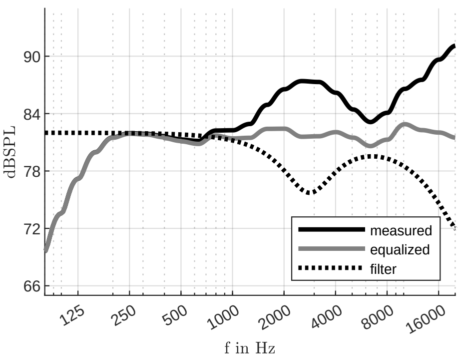

Fig. 3: Third-octave averaged frequency response of one element.

4 Measurements

To measure the frequency response and distortion, a single array element was mounted on a cord in a largely anechoic room ($5\,\text{m} \times 4.2\,\text{m} \times 3\,\text{m}$). Mesaurements were done with an NTI M2230 microphone. Directivity measurements with the same microphones covered an angular grid of $10^\circ \times 10^\circ$, for line arrays suspended from a stand. Measurements concerning coverage over distance also used a suspended line array, and were done in larger lecture hall i9 ($17.25\,\text{m} \times 9.5\,\text{m} \times 3.90\,\text{m}$) of Graz University of Technology, with pressure-zone microphones on the floor to avoid floor reflections.

4.1 Single-element frequency response

As it is not possible to record the free field frequency response directly due to the room dimensions, impulse responses were taken at different distances, 4 cm and 0.5 m. Afterwards, the frequency responses were matched between 400 Hz and 500 Hz. Figure 3 shows the third-octave averaged frequency responses for a single enclosure. Compared to the free field measurement in the data sheet [11], an amplitude boost around 2.5 kHz sticks out. The increase in high frequencies coincides with the on-axis data provided in the data sheet. For equalization, two peak filters were used, $f_{\text{EQ},1} = 2.8\,\text{kHz}$, $g_{\text{EQ},1} = -6\,\text{dB}$, $Q_{\text{EQ},1} = 0.8$ and $f_{\text{EQ},2} = 22\,\text{kHz}$, $g_{\text{EQ},2} = -10.5\,\text{dB}$, $Q_{\text{EQ},3} = 1.69$. After equalization, the direct sound pressure level stays between $\pm 3\,\text{dB}$ for frequencies between 142 Hz and 22 kHz. A stricter limit, $\pm 1.2\,\text{dB}$, increases the lower frequency to 175 Hz.

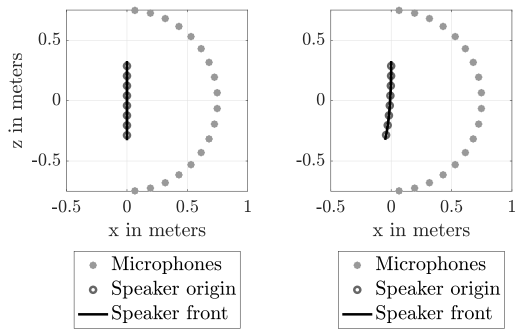

Fig. 4: Setup for directivity data of $\varphi = 0^\circ$, straight array with no angles (left), array optimized for 3 dB per doubling of distance with $\beta = 1/2$ and $g = 0.666$ (right).

4.2 Single-element distortion

To measure distortion of a single element, Room Equalization Wizard[3] was used and the results were exported as text file afterwords for further word. For a single enclosure, Figure 5 shows the fundamental-frequency response to a sinusoid, and the second and the third harmonics as well as total harmonic distortion are shown for a frequency range of 150 Hz to 1.5 kHz, measured at 0.5 m distance to the driver. The results are only shown up to 1.5 kHz, as total harmonic distortion does not increase for higher frequencies and and remains negligibly small. For an A-weighted sound pressure level of 87 dB(A) (left plot), total harmonic distortion rises for low frequencies up to approximately 2%. For frequencies above 250 Hz, it stays below 1%. There is a noticeable peek at 755 Hz, for which mainly the second harmonic distortion of the driver itself contributes to the result. Increasing the volume to 93 dB(A) yields a strong boost in distortion for low frequencies reaching 7%. By contrast, the peak at mid frequencies caused by the driver itself increases only little.

4.3 Single-element directivity

The vertical and horizontal directivity patterns were measured in the acoustically treated measurement chamber of IEM. Four different array configurations (straight; 0 dB/distance doubling, $g = 0.315$, $\beta =$

[3] https://www.roomeqwizard.com/

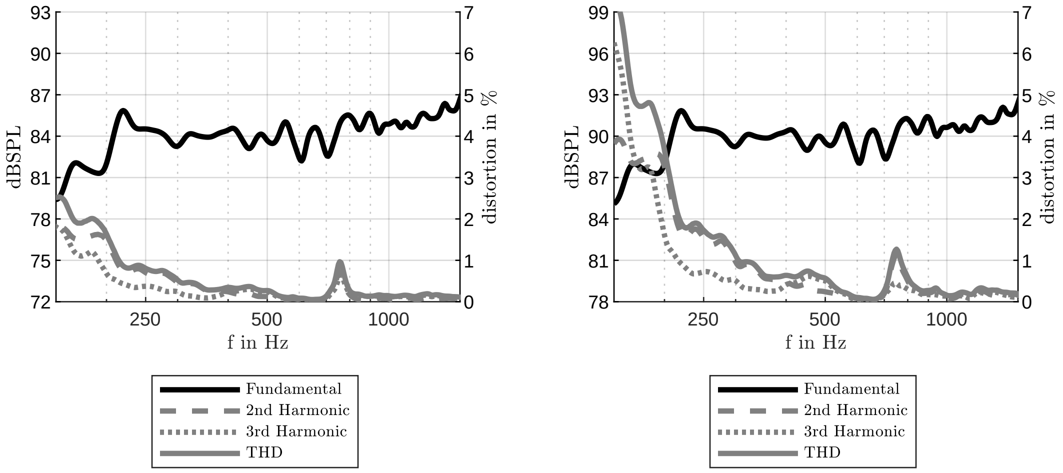

Fig. 5: Fundamental frequency, second, third, and total harmonic distortion of a single enclosure for different sound pressure levels, 87 dB(A) (left) and 93 dB(A) (right).

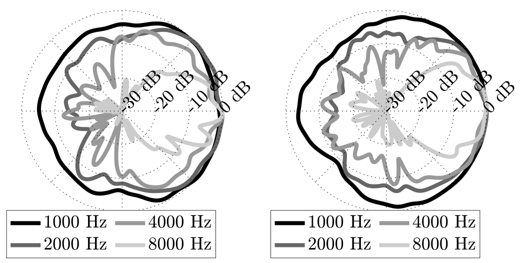

Fig. 6: Directivity pattern of the 5th top element of the straight array, vertical (left), horizontal (right)

0; 1.5 dB/distance doubling, $g = 0.466$, $\beta = 1/4$; 3 dB/distance doubling, $g = 0.666$, $\beta = 1/2$) the array of $N_{\mathrm{ls}} = 8$ elements was set up on a remote-controlled turntable, and the top elements of the line array were aligned with the turntable rotation axis. In a radius of $r_{\mathrm{meas}} = 0.75\,\mathrm{m}$ a total of 18 NTI M2230 measurement microphones are located in a semi-circle from the zenith $\theta = 5^\circ$ in equi-angle spacing of 10° to 175°. The 10° were also chosen as the resolution for the rotation steps of the turntable from an azimuth $\varphi = 0^\circ$ to 350°. By feeding the speakers sequentially using multiple sinusoidal sweeps, $18 \times 36 \times 8$ impulse responses were obtained by the microphones via deconvolution, and truncation to 170 samples at 48 kHz sampling frequency, for brevity of the dataset. This removes reflections from the turntable on the lowest microphone (approx. 60 cm smallest distance between turntable and microphone). For the resulting directivity dataset, Figure 4 sketches the measurement setup for a straight (left) and a curved array for $\beta = 1/2$ and $g = 0.666$.

For interpolated directivity plots of the 5th array element, the measured impulse responses were decomposed into circular harmonics, after removing the linear phase and $1/r$ propagation attenuation in the frequency domain to center the slight off-center location of the element. Figure 6 shows the directivity patterns of this array element interpolated in 1° steps for 4 frequencies. The vertical directivity plot contains the influence of the vertical array extent as slight ripple and increase of the front-to-back ratio, but is otherwise similar to the horizontal directivity, so that we can assume largely axisymmetric loudspeaker directivities. The loudspeakers begin to be directional at 2 kHz and above, and cover a $-6\,\mathrm{dB}$ angle of about $\pm 30^\circ$ at 8 kHz.

Our paper does not pursue analyzing the $10^\circ \times 10^\circ$ directivity data of 3 arrays designs measured further, but datasets are openly accessible, cf. section 7.

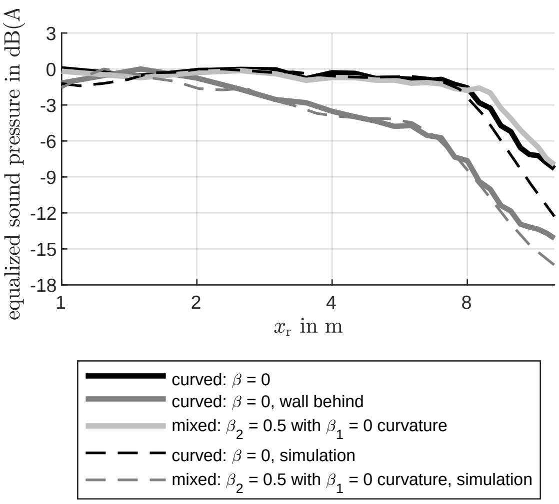

Fig. 7: A-weighted measured sound pressure of a curved array with $\beta = 0$ (solid black) compared to simulation (dashed) as well as the same array mounted in front of a reflecting wall (solid light grey) and mixed array with $\beta_1 = 0$ and $\beta_2 = 0.5$: (dashed dark grey) simulation and measurement (solid dark grey).

4.4 Line array: coverage over distance

In order to record the position-dependent direct sound pressure levels in a room, impulse responses were measured along 22 positions (away from the array, on-axis) starting at $x_r = 1$ m and ending at $x_r = 12.5$ m. Pressure zone microphones were positioned on the ground to prevent floor reflections influencing the measurement. The first 250 samples of the impulse responses (5.2 ms at $f_s = 48$ kHz) were evaluated in a frequency range between 20 Hz and 20 kHz. The impulse responses of the individual loudspeakers are equalized according to the filter presented in Figure 3. Furthermore, for frequencies below the spatial aliasing frequency $f < 4.2$ kHz eq. (5), we applied the typical $\sqrt{f}$ filter required to equalize any line source, cf. Appendix A. The results are averaged in third octaves and the curves are plotted as A-weighted sum.

Figure 7 shows the A-weighted on-axis sound pressure curve for a curved line source with $\beta = 0$ (black solid) compared to the simulation of a discrete source composed of straight-line source polygons of length 6.2 cm with splay angles rounded to integer degrees and leaving gaps in between the discrete elements (black dotted). Furthermore, the results for the same source but mounted in front of a reflecting wall is presented (light grey). The distance between wall and top enclosure was 86 cm and the distance on the bottom was 62 cm.

For the curved arrays with $\beta = 0$ (solid black and solid ligt grey in Figure 7), the direct sound pressure level remains almost constant until 8 m. Due to the finite length and the fact that the differential equation assumes an infinitely long source, the sound pressure level decreases for farther observation points. It is noticeable, that the reflecting wall behind the source does not influence the A-weighted curve of the direct sound level. For the mixed design with $\beta_1 = 0$ for the curvature and $\beta_2 = 0.5$ (solid dark grey in Figure 7), the direct sound level decreases by -3 dB from 1.75 m to 3.5 m, and from 3.5 m to 7 m. For farther observation points, the direct sound level decreases by 6 dB as observed for the curved arrays with $\beta = 0$. Moreover, the measured results almost coincide with the simulated results. The result show that the mixed design is feasible in practise.

5 Conclusion

This paper presented the open design of a miniature line array with 3D-printed enclosures with the practical goal to apply to cinema-sized electroacoustic-music immersive sound reinforcement. Measurements in an anechoic environment showed that the frequency response of the direct sound may be equalized by two simple peak filters and measurements concerning distortion showed that a maximum level of 93 dB(A) can be reached by a single loudspeaker keeping THD below 10%. The results also show the increasing directiviy of a single loudspeaker at higher frequencies. Moreover, we could present that a two-target design based on curving and phasing is feasible in practice.

We plan to undertake psychoacoustic experiments using 8 of the 8-element line arrays surrounding the audience, as a first target application of the hardware presented here. The investigations shall clarify whether mixing balance or envelopment rendering can be improved for an extended audience area in medium-sized immersive sound reinforcement for 50-250 listeners.

6 Acknowledgement

Our research was funded by the Austrian Science Fund (FWF) under project number P 35254-N, Envelopment in Immersive Sound Reinforcement (EnImSo). The authors thank Thomas Musil for his design improvements on our miniature line array, Garcia-Leticia Gabriel, Gregor Schmidt, Niklas Urban, and Chonglian Yu for joint efforts in measuring the coverage over distance (sound reinforcement lab exercise), and Alexander Mülleder and Nico Seddiki for measuring the directivity together (acoustic holography and holophony lab exercise).

7 Data availability

The CAD model of the miniature line array enclosure as well as the measurement data is provided under `https://phaidra.kug.ac.at/o:130608` for download.

References

[1] Ahnert, W. and Noy, D., *Sound Reinforcement for Audio Engineers*, Taylor & Francis Ltd, 2023, ISBN 978-1-032-11518-4.

[2] Zotter, F., Riedel, S., Gölles, L., and Frank, M., "Acceptable Imbalance of Sound-Object Levels for Off-Center Listeners in Immersive Sound Reinforcement," in *Fortschritte der Akustik, DAGA*, Hamburg, 2023.

[3] Gölles, L. and Zotter, F., "Optimally Curved Arc Source for Sound Reinforcement," in *Fortschritte der Akustik, DAGA*, Vienna, 2021.

[4] Riedel, S. and Zotter, F., "Surrounding line sources optimally reproduce diffuse envelopment at off-center listening positions," *JASA Express Letters*, 2(9), p. 094404, 2022, doi:10.1121/10.0014168.

[5] Riedel, S., Gölles, L., Zotter, F., and Frank, M., "Modeling the Listening Area of Envelopment," in *Fortschritte der Akustik, DAGA*, Hamburg, 2023.

[6] Heil, C. and Urban, M., "Sound Fields Radiated by Multiple Sound Sources Arrays," in *92nd AES Conv.*, Vienna, 1992.

[7] Urban, M., Heil, C., and Bauman, P., "Wavefront Sculpture Technology," *J. Audio Eng. Soc*, 51(10), pp. 912–932, 2003.

[8] Straube, F., Schultz, F., Bonillo, D. A., and Weinzierl, S., "An Analytical Approach for Optimizing the Curving of Line Source Arrays," *J. Audio Eng. Soc*, 66(1/2), pp. 4–20, 2018.

[9] Riedel, S. and Zotter, F., "Design, Control, and Evaluation of Mixed-Order, Compact Spherical Loudspeaker Arrays," *Computer Music Journal*, 44, pp. 60–76, 2021, doi:10.1162/comj_a_00581.

[10] Gölles, L. and Zotter, F., "Theory of Continuously Curved and Phased Line Sources for Sound Reinforcement," *Acta Acustica*, accepted 2023.

[11] Acoustics, S., "Product Overview: SB Acoustics 2,5" SB65WBAC25-4 / Aluminum," `https://sbacoustics.com/product/2-5in-sb65wbac25-4/`, 2023.

[12] Skudrzyk, E., *The Foundations of Acoustics: Basic Mathematics and Basic Acoustics*, Springer Link, 1971, ISBN 978-3-7091-8257-4.

A Equalization of an ideal line source

We consider a line source of infinite length that is expanded over the vertical axis z and get its sound pressure by integrating the Green's function over z,

$$p = \int_{-\infty}^{\infty} \frac{e^{-ikr}}{4\pi r} \mathrm{d}z \tag{6}$$

where i denotes the imaginary unit, k the wavenumber and r the distance between source and receiver. By using the Sommerfeld integral for the Hankel function of zero order of the second kind $H_0^{(2)}(kr)$ [12], the pressure becomes

$$p = -\frac{i}{4} H_0^{(2)}(kr)\,. \tag{7}$$

The asymptotic representation for $H_0^{(2)}(kr)$ yields,

$$p \approx \frac{1}{\sqrt{8\pi k}} \frac{e^{-i(kr+\frac{\pi}{4})}}{\sqrt{r}}\,. \tag{8}$$

To equalize the pressure magnitude, the magnitude of the filter has to increase by $\sqrt{f}$.